

Formation of the Silicon Analogues of Isocyanic Acid, HNSiO, and Its Isomers by Neutral–Neutral Reactions of the Fragments: A Computational Study[†]

P. Raghunath, Sanyasi Sitha, K. Bhanuprakash,* and B. M. Choudary

Inorganic Chemistry Division, Indian Institute of Chemical Technology, Hyderabad-500 007, India

Received: May 6, 2003; In Final Form: September 11, 2003

The potential energy surface of [H,N,Si,O] has been generated using the G3B3 methods. Transition states and dissociations have been calculated at the same level. Calculations have also been carried out using ab initio methods at the MP2/6-311+G(d,p) level and the results of the DFT methods (B3LYP/6-31G(d) and G3B3) compared; good agreement between these methodologies was observed, particularly for the optimized geometries and relative energies. On this surface, many intersystem crossings between the singlets and the triplets occur, and the geometries at these crossing points have also been estimated. Finally the reaction coordinates of neutral–neutral reactions of the fragments leading to the stable isomers have been mapped.

Introduction

While isocyanic acid (HNCO) and its sulfur analogues thioisocyanic acid (HNCS) have been identified in interstellar space, the corresponding silicon analogues have not been detected as yet. This is despite the fact that the fragments such as SiO, SiN, OH, NH, NO, SiS, and HNO are present in interstellar space.¹ Given the low-temperature and low-pressure conditions existing there, it would be of interest to understand the possible formation, stability, and fragmentation of the isomers of these silicon species, i.e., [H,N,Si,O]. On the other hand, in the laboratory conditions, the possibility of isolating these isomers has to be understood, and to date only some calculations on the relative stability of the chainlike isomers have been reported.² This then calls for a detailed study of this species, and ideally, the potential energy surfaces (PES) generated for both singlet and triplet multiplicities by computational methods would give an in-depth picture of these isomers. In this regard, the isomers of [H,N,C,O] have been well studied, while for the sulfur analogues only low level calculations of the isomers of [H,N,C,S] have been reported and not the detailed PES.^{3–7} Recently another analogue, namely, the [H,P,C,O] has also been reported.⁸ Though silicon-containing molecules are very important both from the reactions in interstellar space and the semiconductor materials viewpoints, we have not come across any detailed study of the PES or reactions leading to the isomers of [H,N,Si,O].

The main aim of this work is to study the isomerization, stability of the isomers, and neutral–neutral reactions of the fragments leading to the isomers of [H,N,Si,O]. This is achieved by first generating the detailed singlet and triplet PES of the isomers using DFT methodologies. Recent work on silicon species has shown that the widely used B3LYP method with split valence (+polarization/diffuse + polarization) basis sets is quite suitable for geometry and property predictions.^{9,10} Accurate estimation of the energies involving series of single-point calculations on the DFT-optimized geometry, like the G3B3 method, is also carried out to see its effect on the relative

stabilities and isomerization energies. For comparison, the optimization of the isomers in the ab initio MP2 method with further higher-order correlation energy correction obtained by CCSD method at the single-point geometry is also reported. Here we find that, in this work, the computer time consuming MP2 methods and the faster B3LYP method predict almost similar geometries and relative energies in these species. The heat of formation is also estimated using the atomization methods reported in the literature.¹¹ As these molecules in their singlet ground state in some cases dissociate to the spin-forbidden triplet fragments, the minimum energy crossing point (MECP) of the spin isomers has also been determined.¹²

Computational Methods

All the DFT calculations are carried out using the Gaussian98 software package.^{13,14} The optimizations are carried out on all the possible isomers of [H,N,Si,O] and their fragments by the G3B3 method.¹⁵ All geometries are analyzed by harmonic vibrational frequencies obtained at the same level and characterized as minima (no imaginary frequency) or as a transition state (one imaginary frequency). The transition state geometries are then used as an input for IRC calculations to verify the connectivity of the reactants and products.¹⁶ The G3B3 methodology uses the B3LYP/6-31G(d)-minimized geometries as the starting point for the higher-level single-point corrections and also the ZPVE correction based at the same level which differs from the more common G3 method in which the MP2-based geometries and HF-based ZPVE are used. The total energies obtained at 0 K by G3B3 methodology are used to calculate the heat of formation (ΔH_f°). The triplet isomers were obtained using the unrestricted open-shell methods and the spin contamination was found to be very small, with the maximum $\langle S^2 \rangle$ value of 2.08 obtained in only one or two cases. By use of the B3LYP geometries as the starting point, the ab initio MP2/6-311+G(d,p) optimizations were carried out on the isomers. The higher-order correlation energy correction of the MP2 energies was obtained at the single point using the CCSD/6-311G(d,p) method.¹⁷ The details of the results obtained at the B3LYP and CCSD/MP2 levels are given in the Supporting Information.

The MECP has been determined by using an external shell and FORTRAN program developed by Harvey et al.¹⁸ In this

* To whom correspondence should be addressed. E-mail: bprakash@iict.ap.nic.in.

[†] IICT Communication Number: 021113.

TABLE 1: Total Energies (au), Heat of Formation (kcal/mol), Dipole Moments (D), and ZPVE (au) of the Various Singlet and Triplet Isomers of [H,N,Si,O] obtained at the G3B3 level

isomers	G3B3 (0 K)	ΔH_f (0 K) (kcal/mol)	dipole moment (D)	ZPVE
Singlet				
HNSiO (1)	-419.849073 (0.0)	0.2	2.7	0.016214
HNOSi (2)	-419.732838 (72.9)	73.2	2.7	0.016594
HSiNO (3)	-419.755812 (58.5)	58.7	1.1	0.013755
HSiON (4)	-419.691723 (98.7)	99.0	1.1	0.012668
HOSiN (5)	-419.793769 (34.7)	34.9	4.7	0.015681
HONSi (6)	-419.779376 (43.7)	44.0	1.5	0.017964
NSi(H)O (7)	-419.726538 (76.9)	77.1	4.7	0.013095
SiN(H)O (8)	-419.796804 (32.8)	33.0	2.4	0.017486
NO(H)Si (9)	-419.755648 (58.6)	58.8	2.3	0.017374
Triplet				
HNSiO (1)	-419.796901 (0.0)	33.0	3.3	0.014162
HNOSi (2)	-419.714628 (51.6)	84.6	0.7	0.016003
HSiNO (3)	-419.730337 (41.7)	74.7	1.2	0.013211
HSiON (4)	-419.713845 (52.1)	85.1	1.6	0.012066
HOSiN (5)	-419.766520 (19.1)	52.0	1.2	0.015413
HONSi (6)	-419.690211 (66.9)	99.9	1.9	0.016520
NSi(H)O (7)	-419.755721 (25.8)	58.8	2.8	0.013046
SiN(H)O (8)	-419.717286 (50.0)	82.9	2.0	0.017293
NO(H)Si (9)	-419.669114 (80.2)	113.1	2.1	0.016025

method, the MECP geometry is generated using the gradients and electronic energies obtained from Gaussian98 for the two surfaces under the constraint that the difference in the energies and gradients of the two states is minimum.¹⁸

Results and Discussions

Isomers. Both chainlike isomers and branched/cyclic isomers stationary on the singlet and triplet surface of [H,N,Si,O] optimized using G3B3 are reported with details such as total energies in Table 1 and geometries in Figures 1 and 2. The PES has about nine stationary points on the singlet and an equal number on the triplet surface, all of which have been characterized as minima by analyzing the vibrational frequencies. It should be noted that though there are some higher energy isomers in some connectives, we report here only those that are the lowest in energy at that particular connectivity. By comparison of the structures of the other 16 valence electron systems, such as HNCS, HPCO, or HNCO, with the structures of these isomers, it is found that they are almost similar, with the chainlike isocyanic isomer with NH (or PH) connectivity being the most stable isomer, i.e., HNSiO, HNCO, HNCS, or HPCO.²⁻⁷ The dihedral angles in the most stable isomers are almost equal except in the phosphorus analogue where a bond angle of less than 90° was obtained for the angle HPC.⁸ There are about six chain isomers and three ring isomers (classified based on bond angles) in the singlet case and an equal number of chain isomers in the triplet. But in the case of triplet, only one cyclic structure turned out to be a stationary point, the others are branched with a large NSiO or SiNO bond angle. The singlet isomers, with the exception of **8** and **9**, are planar, while the triplets **1**, **5**, and **9** turn out to be nonplanar.

The relative energies are calculated with respect to the most stable isomer in the respective spin symmetry. The energies obtained by CCSD/MP2 are compared with the B3LYP (both in Supporting Information) and with the more accurate G3B3 values (Table 1). Our discussion will be limited to some of the lowest isomers, while the table gives details of all the calculated isomers. The lowest (global minima) predicted isomer by all the methods is isomer **1**, while within the individual spin symmetries, isomer **1** also happens to be the lowest. The next low-lying singlet isomer is **8**, which can be described as the

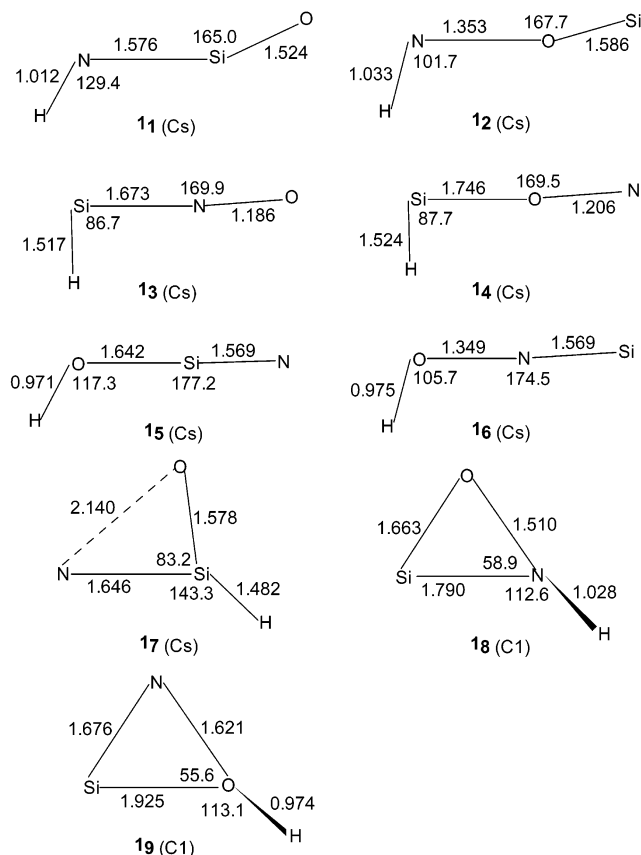


Figure 1. Equilibrium geometries in the singlet state of the [H,N,Si,O] system, optimized at the B3LYP/6-31G(d) (G3B3 geometries) level. Bond lengths are in angstroms and angles in degrees.

cyclized isomer of **1**. This lies about 25 kcal/mol above the lowest isomer as predicted by the B3LYP/6-31G(d) calculation and around 28.3 kcal/mol as predicted by CCSD/MP2 methods. The G3B3 raises the energy a little higher to a value of 32.8 kcal/mol. In the case of triplets, it is the isomer **5** which is the next most stable isomer. Here, the predicted values by both the methods are 11.5 kcal/mol by the B3LYP and 11.7 kcal/mol by the CCSD/MP2 methods. Again G3B3 raises the relative energy difference to 19.1 kcal/mol. The next two low-lying isomers **5** and **6** in the singlet symmetry are almost degenerate in energy in the CCSD/MP2 method and with ZPVE correction become equal. In the B3LYP case, an energy difference of 3.8 kcal/mol is seen even with the ZPVE correction. This energy gap slightly increases when the G3B3 corrections are taken into account and indicates up to a 9 kcal/mol difference. In the case of triplets, the next low-lying isomer is **7**, which is a branched isomer. The relative energies obtained are 16 and 25.8 kcal/mol for the B3LYP and the G3B3, respectively. The isomer **3**, the next higher energy isomer lies about 19 kcal/mol above isomer **3** in the B3LYP and MP2 methods while the corrections due to G3B3 increase it to 41 kcal/mol. Overall, both DFT and ab initio methods with the correlation energy correction seem to have a good agreement in geometries and relative energies.

The calculated heats of formation are also shown in Table 1. These are based on the G3B3 enthalpies at 0 K. In general, the singlets have a lower heat of formation (as expected) with HNSiO having a heat of formation of 0.2 kcal/mol. The triplet isomer has a heat of formation of 33.0 kcal/mol.

PES. Interconversions between the isomers can be broadly divided into three types, cyclization (or ring opening), 1,2 H migration, 1,3 H migration, and sometimes combinations between these. The potential energy surfaces generated by the

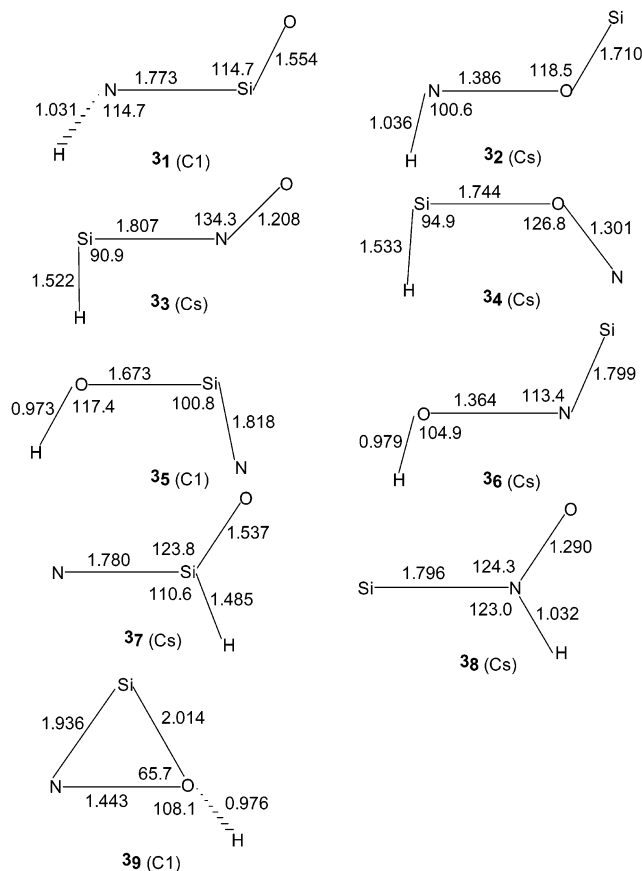


Figure 2. Equilibrium geometries in the triplet state of the [H,N,-Si,O] system, optimized at the B3LYP/6-31G(d) (G3B3 geometries) level. Bond lengths are in angstroms and angles in degrees.

G3B3 methods for the singlets and the triplet isomers are shown in Figures 3 and 4, respectively. The relative energies are indicated in the figures with respect to the most stable isomer. The transition-state energies for both singlets and triplets are tabulated in Table 2, while the frequencies for the transition states obtained by the same method are tabulated in the Supporting Information. The transition state geometries obtained are shown in Figures 5 and 6.

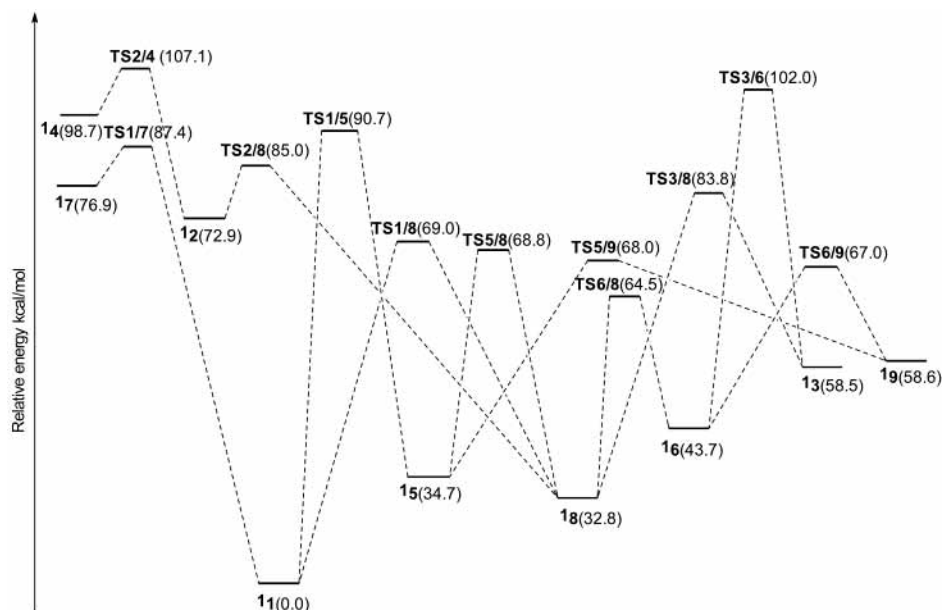


Figure 3. Singlet potential energy surface of [H,N,Si,O] system at G3B3 level of theory. Relative energies (kcal/mol) are given in parentheses.

TABLE 2: Total Energy (au) of the Singlet and Triplet Transition States for the Isomerizations in [H,N,Si,O] Calculated Using G3B3

singlet		triplet	
transition states	G3B3	transition states	G3B3
TS ¹ 1/ ⁵	-419.704601	TS ³ 1/ ⁵	-419.734428
TS ¹ 1/ ⁷	-419.709765	TS ³ 1/ ⁷	-419.710018
TS ¹ 1/ ⁸	-419.739057	TS ³ 2/ ⁴	-419.679837
TS ¹ 2/ ⁴	-419.678456	TS ³ 2/ ⁸	-419.704027
TS ¹ 2/ ⁸	-419.713818	TS ³ 2/ ⁹	-419.641319
TS ¹ 3/ ⁶	-419.686542	TS ³ 3/ ⁶	-419.667884
TS ¹ 3/ ⁸	-419.715541	TS ³ 3/ ⁸	-419.677847
TS ¹ 5/ ⁸	-419.739509	TS ³ 5/ ⁷	-419.687667
TS ¹ 5/ ⁹	-419.740778	TS ³ 5/ ⁹	-419.655201
TS ¹ 6/ ⁸	-419.746217	TS ³ 6/ ⁸	-419.615481
TS ¹ 6/ ⁹	-419.742232	TS ³ 6/ ⁹	-419.659253
TS/dis(¹ 4)	-419.658223	TS/dis(³ 1)	-419.662138
TS/dis(¹ 7)	-419.676380	TS/dis(³ 2)	-419.699944
		TS/dis(³ 6)	-419.642902
		TS/dis(³ 8)	-419.676109
		TS/dis(³ 9)	-419.635712

Singlet isomer **1** can isomerize to **8** by cyclization. The transition state of the isomerization between **1** and **8** is nonplanar, and the cyclization takes place with the formation of an N–O bond. This process requires 66.6 kcal/mol by the B3LYP method, and the usage of the more accurate G3B3 increases the barrier to 69 kcal/mol. Here, the energy difference between the two methods is only around 2.4 kcal/mol. **1** can also isomerize to **15** and **17** through hydrogen migration. The transition state ¹1/⁷ is a planar molecule which is a 1,2 H migration. This is predicted to be of high energy with a difference of 6 kcal/mol for the two methods. The 1,3 H migration to **15** requires a higher activation energy of around 96.9 kcal/mol by the B3LYP method and the G3B3 predicts around 6.2 kcal/mol less.

The next lowest isomer **18** can undergo two types of ring opening reactions. The ring opening with breaking of the N–O bond leads to **11**, with a barrier of 36 kcal/mol. The ring opening by breaking the N–Si bond leads to **12**, and this has a barrier of 48 kcal/mol, the G3B3 method increases the barrier to 52.2 kcal/mol. H migration from N to O, followed by ring opening, leads to **15** and requires an energy of around 38 kcal/mol, while the G3B3 energy decreases this to 36 kcal/mol. H migration from N to Si followed by ring opening leads to isomer **13** with

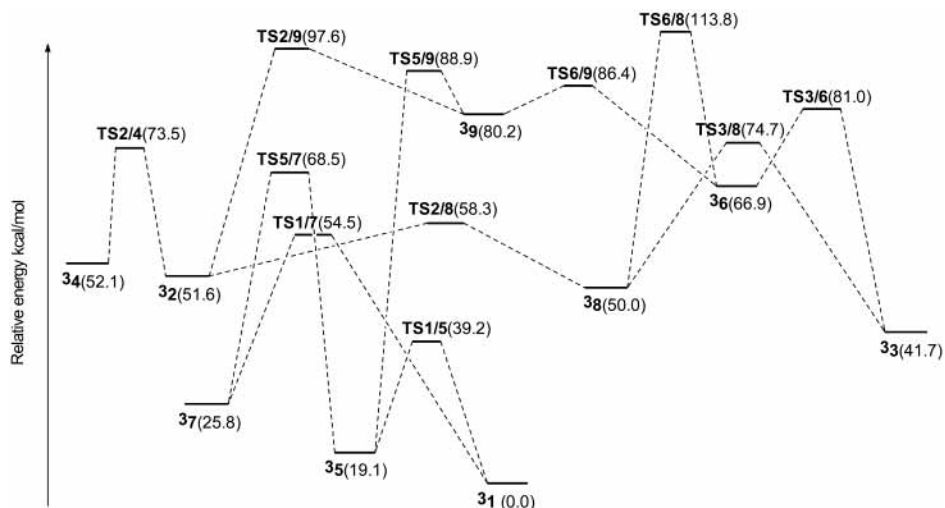


Figure 4. Triplet potential energy surface of [H,N,Si,O] system at G3B3 level of theory. Relative energies (kcal/mol) are given in parentheses.

TABLE 3: Total Energy (au) of the Fragments Calculated at G3B3 Level

fragments	G3B3	fragments	G3B3
¹ NH	-55.127283	³ HNO	-130.383604
³ NH	-55.193914	¹ HON	-130.345268
² OH	-75.696367	³ HON	-130.372493
² NO	-129.836250	l- ² NSiO	-419.163465
² SiH	-289.837711	² NOSi	-419.097697
¹ SiO	-364.558551	c- ² NSiO	-419.163900
³ SiO	-364.409488	² SiNO	-419.163614
² SiN	-343.960269	¹ Si	-289.195544
¹ HNSi	-344.658047	³ Si	-289.223010
³ HNSi	-344.528206	² H	-0.501087
¹ HSiN	-344.555539	² N	-54.471734
³ HSiN	-344.511388	⁴ N	-54.565162
² HSiO	-365.092206	¹ O	-74.957092
² HOSi	-365.105323	³ O	-75.032293
¹ HNO	-130.412519		

a barrier of around 45 kcal/mol and, by the G3B3, 51 kcal/mol. **18** can also simultaneously undergo the combination of ring opening and H migration to O which lead to **16** with a low barrier of 33.4 kcal/mol, and the higher order corrections decrease this to 31.7 kcal/mol.

Isomer **15** can cyclize to **19**, which requires only 26.4 kcal/mol, and the effect of the higher-order corrections improve this energy by only 6.9 kcal/mol. The H migration to N, isomerizing to **11**, requires an activation energy of 56 kcal/mol, and the isomerization of **15** to **18** requires a much lower energy of 34.1 kcal/mol. Isomer **16** can undergo cyclization to **19** requiring only around 23.3 kcal/mol. A four-membered ring transition state and an activation energy of 58.3 kcal/mol is required for the isomerization of **16** to **13**. This is a 1,3 H migration; hence, more energy is required. The isomerization of **16** to **18** requires around 20.8 kcal/mol and is of lower barrier. Isomer **12** can convert to **14** by 1,3 H migration, and accordingly the transition state is a four-membered ring, and the activation energy required for this migration is 40.2 kcal/mol by the B3LYP method and around 35 kcal/mol for the G3B3 methods. Ring opening of **19** to **16** requires an activation energy of only 8.4 kcal/mol. On this surface, we were unable to locate the transition states for isomerization of **12** to **19**, **13** to **17**, and **15** to **17**. Two other transition states that involve isomer **14**, which are of very high energy, have not been located.

In the PES of the triplets, the overall picture is that the isomerizations are predicted to have smaller activation energies than the singlet. Isomer **31** can isomerize to **35** through 1,3 H migration, which requires only 27.4 kcal/mol by the B3LYP

method. Here the G3B3 calculations show that the activation energy is substantially higher for this isomerization and is around 39 kcal/mol. **31** requires around 54.5 kcal/mol for the 1,2 H migration leading to the isomer **37**. But we were unable to locate the transition state to **38**, unlike in the singlet case. Isomer **35** isomerizes to the branched isomer **37** via a 1,2 H migration, which requires 54.3 and 49.5 kcal/mol by both methods, respectively. This transition state did not converge in the singlet case. There is no isomerization of **35** to **38** as observed in the singlets, as the isomer **8** in the triplet case is not cyclic but branched. **35** can cyclize to **39**, the only cyclic molecule in the triplets, and it requires 70 kcal/mol. The branched isomer **38** can isomerize to the chain isomer **32** via the low-lying transition state, which requires only 8.3 kcal/mol. The isomer **38** can also isomerize to **33**, which is also a 1,2 H migration, but this time the H migrates to the Si and requires only 24.7 kcal/mol with a difference of 1 kcal/mol between the two methods. Overall in both singlets and triplets, the more stable isomers show small changes in relative energies with the inclusion of the higher-order single-point calculations (G3B3) to the basic B3LYP/6-31G(d) level.

MECP. The crossing of the triplet and the singlet surfaces that are bound at some lowest point (MECP) is sometimes considered as the transition point for the intersystem crossing.³ The MECP geometries have been determined for the isomers at the B3LYP/6-31G(d) (G3B3 geometries) level; these are shown in Figure 7. Isomers **4** and **7** do not have a crossing point as the triplet states are the ground states and the dissociation to the triplet fragments are lower than the singlet dissociations. The idea of finding out the geometry of MECP is to understand the most feasible pathway the reaction would take when the two fragments of different spins interact. The fragments can undergo side-on addition (to form a chainlike isomer) or an insertion-type (to form a branched/ring isomer) reaction on collisions to form either the singlet or the triplet isomer. The relative energies discussed below are without the inclusion of the higher-level corrections.

Two low-lying reaction coordinates, namely, the ³NH + SiO and HNSi + ³O, could contain the MECP for the formation of isomers **1**. **MECP-1** (singlet-triplet crossing point on the surface of **1**) lies around 32.7 kcal/mol above the singlet. The N-Si bond is elongated and indicates the proximity to the dissociation to fragments NH and SiO. This indicates clearly that this MECP point lies on the ³NH + SiO reaction surface. The **MECP-1** lies only 0.8 kcal/mol above the triplet isomer.

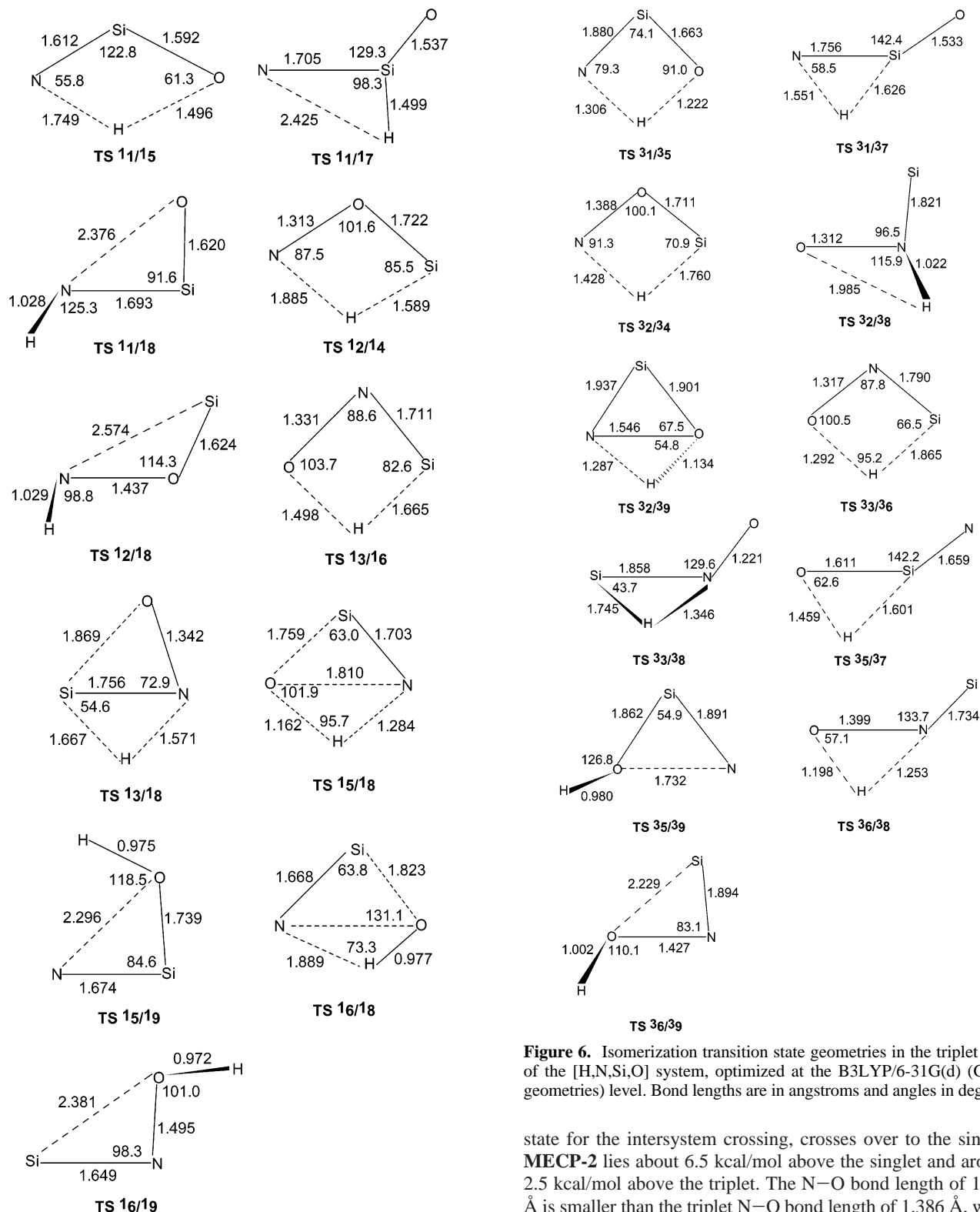


Figure 5. Isomerization transition state geometries in the singlet state of the [H,N,Si,O] system, optimized at the B3LYP/6-31G(d) (G3B3 geometries) level. Bond lengths are in angstroms and angles in degrees.

This small energy difference and the similarity in geometry may suggest that the triplet can be formed in some instances. The crossing point lies around 21.8 kcal/mol below the dissociation channel (fragment energies are given in Table 3 and geometries in Figure 8). For the second reaction coordinate, we were unable to locate the MECP, indicating that in this reaction, ³1 is formed first; this then via the **MECP-1**, which now acts as the transition

Figure 6. Isomerization transition state geometries in the triplet state of the [H,N,Si,O] system, optimized at the B3LYP/6-31G(d) (G3B3 geometries) level. Bond lengths are in angstroms and angles in degrees.

state for the intersystem crossing, crosses over to the singlet. **MECP-2** lies about 6.5 kcal/mol above the singlet and around 2.5 kcal/mol above the triplet. The N–O bond length of 1.374 Å is smaller than the triplet N–O bond length of 1.386 Å, while the Si–O bond length of 1.659 Å is also smaller than the 1.710 Å in the triplet. The bond lengths of the MECP geometry are longer than the corresponding ones in the singlet, indicating that the MECP geometry is an intermediate between the singlet and triplet geometry and not near the dissociation channel. The lowest dissociation channel is the ³NH + OSi, and the triplet's geometry is very close to this. These fragments then would form ³2 via the transition state (**TS/dis**(³2)) shown in Figure 9, which has a barrier around 10.9 kcal/mol. The MECP then can be inferred to lie on the reaction coordinate of the O–Si bond stretching and is the intersystem crossing for ³2 to ¹2 isomers.

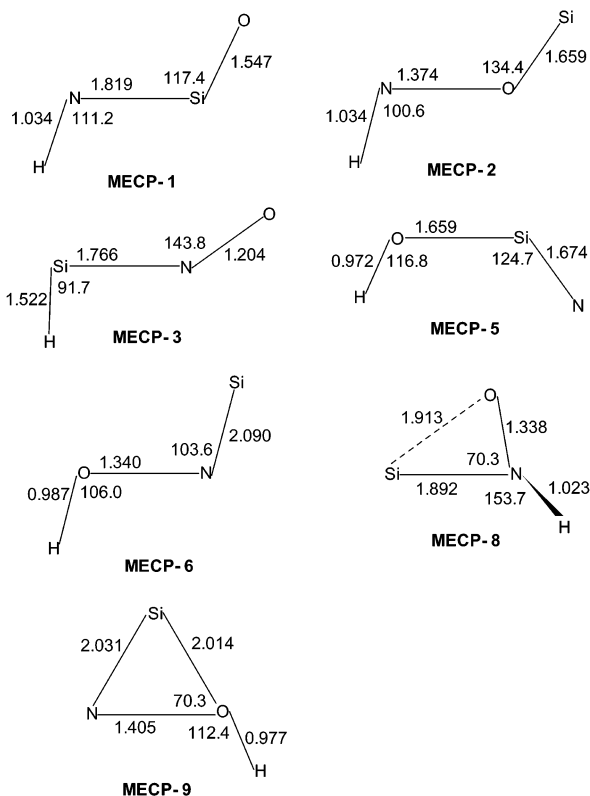
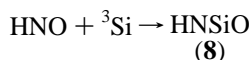
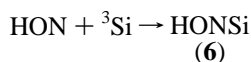
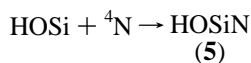
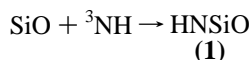


Figure 7. Geometries at the MECP for various isomers in the [H,N,Si,O] system optimized at the B3LYP/6-31G(d) (G3B3 geometries) level. Bond lengths are in angstroms and angles in degrees.

MECP-3 lies around 0.9 kcal/mol above the triplet and 8.4 kcal/mol above the singlet, and it lies between the singlet and triplet; hence, it can also be considered as the transition state for the intersystem crossing rather than for dissociation. The geometry of **MECP-5** is closer to the dissociation to the fragments which involves ^4N , which also happens to be the lowest channel for dissociation. This MECP lies 4.6 kcal/mol above the triplet and 10.2 kcal/mol above the singlet. **MECP-6** is clearly close to the dissociation to the ^3Si and HON fragments. But the lowest channel of dissociation for this isomer is ^2H and $^2\text{ONSi}$ for both singlet and triplet. The crossing point lies about 11.4 kcal/mol above the triplet and 59.5 kcal/mol above the singlet. The next two isomers are rings **8** and **9**; **MECP-8** is very close to the triplet lying only 0.2 kcal/mol above it, while the singlet is about 35.8 kcal/mol lower. The geometry suggests that it is closer to the dissociation to ^3Si and HNO. **MECP-9** indicates that the crossing point lies lower than the fragments HON and ^3Si energy and above the triplet by 2.4 kcal/mol and above the singlet by 46.5 kcal/mol. On the basis of the above discussions, we can infer that the MECPs lying on the dissociation channels are



Reactions. $^2\text{OH} + ^2\text{SiN}$. The side-on addition reaction of $^2\text{-OH}$ with ^2SiN can give rise to isomer **5** either in the singlet or

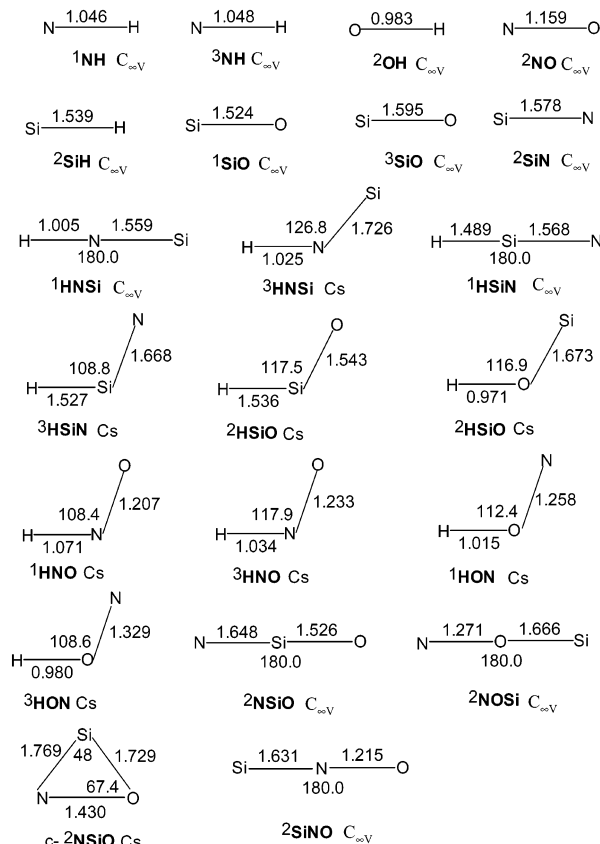


Figure 8. Optimized geometries of fragments at B3LYP/6-31G(d) (G3B3 geometries) level. Bond lengths are in angstroms and angles in degrees.

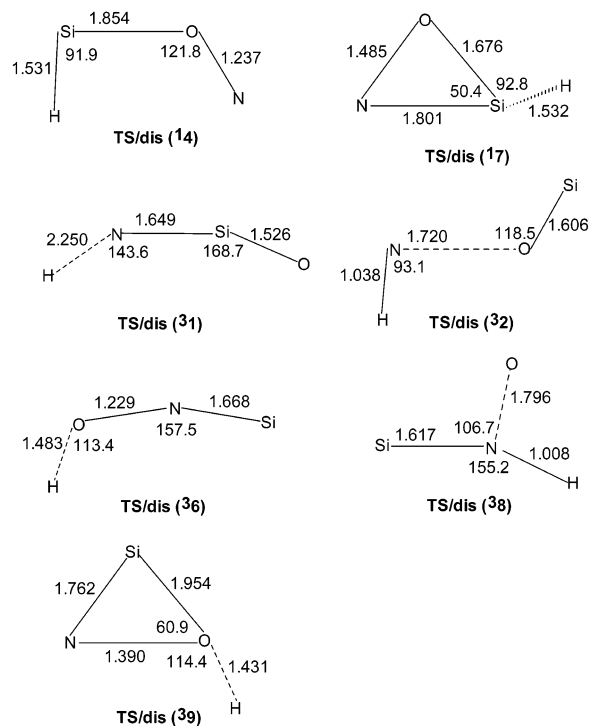
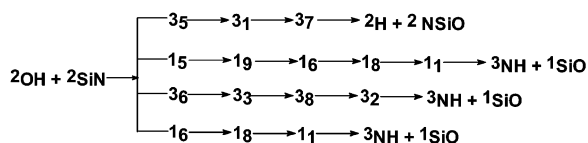


Figure 9. Dissociation transition state geometries in the singlet and triplet state of the [H,N,Si,O] system, optimized at the B3LYP/6-31G(d) (G3B3 geometries) level. Bond lengths are in angstroms and angles in degrees.

triplet form if the reaction proceeds with the bond formation of Si–O or to singlet or triplet **6** with the bond formation between

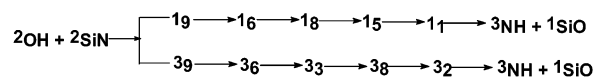
N and O. Of the 4 possible pathways, i.e.,



the one that forms **15** is the most exothermic one releasing 86.1 kcal/mol. The lowest dissociation of **15** to $^2\text{SiOH}$ and ^4N requires an energy of 77.0 kcal/mol, while its isomerization to **19** requires a much lower energy of 33.3 kcal/mol as the activation. The isomerization of **15** to **19** is an endothermic process with a critical energy of 23.9 kcal/mol. If **15** isomerizes to **18** (slightly higher barrier energy), then the barrier is 34.1 kcal/mol, but the isomerization itself is a exothermic process with a release of 2 kcal/mol. The isomerization from **19** to **16** is exothermic with a release of 15 kcal/mol. The dissociation of **19** and **16** requires high energy, and the dissociation of **16** to its lowest dissociation channel is $^2\text{H} + ^2\text{ONSi}$ (72.0 kcal/mol). **18** energetically prefers isomerization, rather than dissociation, to **11** with a barrier of 36.2 kcal/mol and releasing 33 kcal/mol by the G3B3 method. **11** can finally dissociate to ^3NH and ^1SiO passing through the **MECP-1**. The transition state for the dissociation of **31** did not converge with the normal options in the B3LYP method (G3B3) and with relaxed convergence criteria optimized to a very long N–Si bond. At a shorter N–Si bond length, the transition state obtained was for the dissociation to NH^+ and SiO^- . This is because the spin densities in this state obtained were suggestive of one electron each on N and Si. Carrying out the calculations with a much higher basis set such as 6-311++G(d,p) at the B3LYP level did not make any difference. We carried out the calculations for this dissociation using the MP2 method and this yielded a dissociation energy of around 2–3 kcal/mol with spin densities on N (1.9) and a bond length of 2.374 Å for the N–Si bond. This predicts a transition state for dissociation which lies after the **MECP**. It should be noted that the position of the **MECP-1** being before the transition state of **31** dissociation, the **11** endothermically dissociate to ^3NH and SiO or it can also cross over to **31** via the crossing point and then dissociate to the next lowest fragmentation $\text{HNSi} + ^3\text{O}$ endothermically. Overall, the route is exothermic with the final products lying below the reactants, and all the transition states are also below the reactants. This reaction is feasible in the interstellar conditions with most probable products being ^3NH and SiO. The second route with the formation of **16** is exothermic by 77 kcal/mol. All the dissociations on this reaction pathway require very high energy while the isomerizations much less. This also finally leads to $^3\text{NH} + \text{SiO}$ as the most probable products.

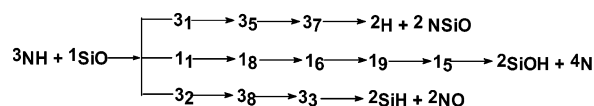
The side-on addition can also yield the triplet isomers **5** and **6**. Here the formation of **5** is more exothermic. The isomerization to **31** from **35** requires an activation energy of 19 kcal/mol, while the lowest dissociation requires 60.3 kcal/mol. On the other hand the isomerization from **31** to **37** is highly endothermic, while the dissociation of **31** to ^3NH and SiO passes through a small barrier predicted only by the MP2 methods. Finally **37** is very stable against dissociation, requiring 57.2 kcal/mol for the same. The reaction proceeding through the other triplet, i.e., **6**, requires very little energy for dissociation to ^2H and $^2\text{ONSi}$, while the isomerization to **33** requires around 14.1 kcal/mol. **33** can dissociate to SiH and NO, which is competitive with isomerization to **38**. The isomerization to **32** requires very little energy and so is the dissociation of **32** to ^3NH and SiO. Again, the lowest channel in the triplet route is the dissociation to $^3\text{NH} + \text{SiO}$.

The other possible reaction is the insertion, and it can take the following pathways, i.e.,



The possible isomers are the singlet and triplet **9**, which form without any barrier energy, of which the formation of **19** is highly exothermic and has a value of 62 kcal/mol. The main notable feature of this pathway (singlet) is the high dissociation energies and comparatively lower isomerization energies, and the lowest-energy pathway through the singlet yields the **11** isomer. The isomerization of **18** to **11** is exothermic by around 33 kcal/mol, while **18** to **15** is predicted to be endothermic by 5 kcal/mol. But the barrier for the latter isomerization is lower by 5 kcal/mol. $^3\text{NH} + ^1\text{SiO}$ seem to be the most common products as the reaction is overall exothermic. The triplet route also turns out to be exothermic.

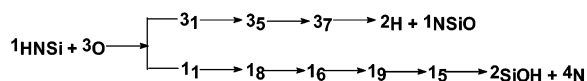
$^3\text{NH} + ^1\text{SiO}$. The other possible diatomic fragments which can react is the one involving ^3NH and SiO by the following pathways



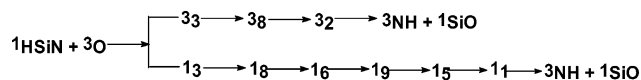
Here the addition reactions yield only three pathways, namely, the singlet and triplet **1** and only triplet **2**. On the basis of the geometry and energy of **MECP-2**, it can be seen that for the singlet to be formed, the reactants should take the path **TS/dis-(32)** \rightarrow **32** \rightarrow **MECP-2** \rightarrow **12**. The **12** turns out to be higher in energy than the reactants, and we were unable to locate any transition state. It should be also kept in mind that the **MECP-2** is higher in energy than both the singlet and the triplet and hence acts as a transition state for the intersystem crossing. The **32**, though higher in energy than the reactants, requires an activation energy of 33.0 kcal/mol to be formed from the reactants, and the reaction is endothermic. The pathway to the singlet **11** passes through the small barrier predicted by the MP2 method and then passes through the **MECP-1** before it forms either the singlet or the triplet **1**. The dissociation of **11** to ^2H and $^2\text{NSiO}$ is very highly endothermic and the isomerization to **18** is also a very high energy process. On the other hand, the triplet requires relatively less energy to cross the barrier and isomerize to **35**. The dissociation of **11** to $\text{HNSi} + ^3\text{O}$ is via **31** (vide supra). Basically the addition of these fragments is an endothermic process, but once the reaction proceeds, only isomer **1** forms. The only feasible pathway for the insertion reaction proceeds through the endothermic pathway to **38** and hence does not gain enough energy to cross the barrier for isomerization, intersystem crossing to **18**, or for dissociation through the lowest path.

$^1\text{HNSi} + ^3\text{O}$, $^1\text{HSiN} + ^3\text{O}$, and $^1\text{HNO} + ^3\text{Si}$. Next we focus on the reaction pathways of the triplet O with the triatomic HNSi and HSiN. The possible existence of HNSi/HSiN has been discussed by Parisel et al.,¹⁹ hence the reactions of these fragments with ^3O along with the reaction of HNO with ^3Si are also studied. The reaction pathway for the addition can proceed without a barrier to the triplet state, but for the singlet to form it has to be via the triplet **1** then via the crossing point **MECP-1** to form the isomer **11**. As the crossing point lies before the transition state, the triplet isomer is required to cross the **MECP-1** before it goes downhill for the formation of the singlet **1**. Thus the lower-energy triplet route would prefer the formation of **11**. In the insertion pathway (**38** \rightarrow **32** \rightarrow $^3\text{NH} + ^1\text{SiO}$), the

reaction to form the triplet isomer **8** is exothermic but has to cross the barrier, and the dissociations and the isomerization in this route are higher energy process.



The reaction pathway passes through the crossing point **MECP-3**, (which acts as the transition state) before they can cross over to singlet from the triplet state. The formation of **11** is the larger exothermic reaction.



The possible pathway of O being inserted into the triatomic fragment HSiN is ${}^3\text{7} \rightarrow {}^3\text{1} \rightarrow {}^3\text{5} \rightarrow \text{2SiOH} + \text{4N}$. It should be noted that **37** is the ground state, and hence the spin crossing does not occur here. The insertion is exothermic by as much as 105.4 kcal/mol and, if the low-energy path is to be taken, proceeds with isomerization to **31**.

The reaction pathways of the reaction between HNO and ${}^3\text{Si}$ are as follows, i.e., ${}^3\text{2} \rightarrow {}^3\text{8} \rightarrow {}^3\text{3} \rightarrow \text{2SiH} + \text{2NO}$. The addition reaction proceeds through the triplet isomer with a large gain in energy of 49.6 kcal/mol, which can dissociate to ${}^3\text{NH}$ and SiO or isomerize to **38**, both of which are low-energy process. The isomerization of **38** to **33** is a low-energy process and competitive between the isomerization and the dissociation. The insertion pathway prefers the formation of **11** and its dissociation products. The detailed reaction pathways are given in the Supporting Information.

Conclusions

Silicon analogues of the isocyanic acid and its isomers have been investigated by computational methods. Both *ab initio* at MP2 and G3B3 at the DFT level indicate that there as many as nine stationary states on the singlet surface and an equal number on the triplet surface, which have been characterized as minima. The dissociations and the isomerizations require high energies, indicating that these isomers are quite stable and in some conditions can be detected in the laboratory. The neutral–neutral reactions on this surface mapped using the fragments reveal that though many of them are barrierless, they are exothermic enough to dissociate to other lower channels. These indicate that in the interstellar space the possibility of detecting HNSiO formed from the neutral–neutral reactions is not very high but the possibility of the formation of the stable isomer from neutral–ion reactions is not ruled out. We are right now in the process of mapping the neutral–ion reactions of this surface.

Acknowledgment. We thank Dr. K. V. Raghavan, Director, IICT, for his constant support and Dr. R. Srinivas for the useful discussions in this work.

Supporting Information Available: Tables of total and relative energies and harmonic vibrational frequencies and IR intensities of the singlet and triplet isomers, figures of equilibrium geometries of the singlet and triplet states of the [H,N,-Si,O] system optimized at the MP2/6-311+G(d,p) level, and detailed reaction pathways of product formation. This material is available free of charge via the Internet at <http://pubs.acs.org>.

References and Notes

- (1) Devienne, F. M.; Barnabe, C.; Couderc, M.; Ourisson, G.; C. R. *Acad. Sci. Paris, Ser. II C* **2000**, 3, 341 (b) Wootten, H. A. The 121 reported interstellar and circumstellar molecules. Complete to 1/1/01. <http://www.cv.nrao.edu/~awootten/allmols.html>.
- (2) Junker, M. Matrixisolation Subvalenter Siliciumverbindungen. Doctoral dissertation. Universitat Karlsruhe, 1999.
- (3) Mabel, A. M.; Luna, A.; Lin, M. C.; Morokuma, K. *J. Chem. Phys.* **1999**, 105, 6439.
- (4) Shapley, W. A.; Bacskay, G. B. *J. Phys. Chem. A* **1999**, 103, 6624.
- (5) Tao, Yu-guo; Ding, Yi-hong; Li, Ze-sheng; Huang, Xu-ri; Sun, Chia-Chung. *J. Phys. Chem. A* **2001**, 105, 3388. (b) Yokoyama, K.; Takane, Shin-ya; Fueno, T. *Bull. Chem. Soc. Jpn.* **1991**, 64, 2230.
- (6) Wierzejewski, M.; Mielke, Z. *Chem. Phys. Lett.* **2001**, 349, 227.
- (7) Bak, B.; Christiansen, J. J.; Nielsen, O.; Svanholt, H. *Acta Chem. Scand. Ser. A* **1977**, 31, 666.
- (8) Fu, Hong-gang; Yu, Hai-tao; Chi, Yu-juan; Li, Ze-sheng; Huang, Xu-ri; Sun, Chia-Chung. *Chem. Phys. Lett.* **2002**, 361, 62.
- (9) Srikanth, R.; Bhanuprakash, K.; Srinivas, R. *Chem. Phys. Lett.* **2002**, 360, 294.
- (10) Ding, Yi-hong; Li, Ze-sheng; Huang, Xu-ri; Sun, Chia-Chung. *J. Phys. Chem. A* **2001**, 105, 5896.
- (11) Nicolaides, A.; Rauk, A.; Glukhovtsev, M. N.; Radom, L. *J. Phys. Chem.* **1996**, 100, 17460.
- (12) (a) Stevens, J. E.; Cui, Q.; Morokuma, K. *J. Chem. Phys.* **1998**, 108, 1544. (b) Luna, A.; Mabel, M.; Morokuma, K. *J. Chem. Phys.* **1996**, 105, 3187.
- (13) Frisch, M. J.; Trucks, G. W.; Schlegel, H. B.; Scuseria, G. E.; Robb, M. A.; Cheeseman, J. R.; Zakrzewski, V. G.; Montgomery, J. A., Jr.; Stratmann, R. E.; Burant, J. C.; Dapprich, S.; Millam, J. M.; Daniels, A. D.; Kudin, K. N.; Strain, M. C.; Farkas, O.; Tomasi, J.; Barone, V.; Cossi, M.; Cammi, R.; Mennucci, B.; Pomelli, C.; Adamo, C.; Clifford, S.; Ochterski, J.; Petersson, G. A.; Ayala, P. Y.; Cui, Q.; Morokuma, K.; Malick, D. K.; Rabuck, A. D.; Raghavachari, K.; Foresman, J. B.; Cioslowski, J.; Ortiz, J. V.; Stefanov, B. B.; Liu, G.; Liashenko, A.; Piskorz, P.; Komaromi, I.; Gomperts, R.; Martin, R. L.; Fox, D. J.; Keith, T.; Al-Laham, M. A.; Peng, C. Y.; Nanayakkara, A.; Gonzalez, C.; Challacombe, M.; Gill, P. M. W.; Johnson, B. G.; Chen, W.; Wong, M. W.; Andres, J. L.; Head-Gordon, M.; Replogle, E. S.; Pople, J. A. *Gaussian 98*, revision A.9; Gaussian, Inc.: Pittsburgh, PA, 1998.
- (14) (a) Becke, A. D. *J. Chem. Phys.* **1993**, 98, 5648. (b) Lee, C.; Yang, W.; Parr, R. G. *Phys. Rev. B* **1988**, 37, 785.
- (15) Baboul, A. G.; Curtiss, L. A.; Redfern, P. C.; Raghavachari, K. *J. Chem. Phys.* **1999**, 110, 7650.
- (16) (a) Gonzalez, C.; Schlegel, H. B. *J. Chem. Phys.* **1989**, 90, 2154. (b) Gonzalez, C.; Schlegel, H. B. *J. Phys. Chem.* **1990**, 94, 5523.
- (17) (a) Cizek, J. *Adv. Chem. Phys.* **1969**, 14, 35. (b) Purvis, G. D.; Bartlett, R. J. *J. Chem. Phys.* **1982**, 76, 1910. (c) Scuseria, G. E.; Janssen, C. L.; Schaefer, H. F., III. *J. Chem. Phys.* **1988**, 89, 7382. (d) Scuseria, G. E.; Schaefer, H. F., III. *J. Chem. Phys.* **1989**, 90, 3700.
- (18) Harvey, J. N.; Aschi, M.; Schwarz, H.; Koch, W. *Theor. Chem. Acc.* **1998**, 99, 95.
- (19) Parisel, O.; Hanus, M.; Ellinger, Y. *J. Phys. Chem. A* **1997**, 101, 299.